Virchows Arch [Pathol Anat] (1983) 398:329–346

Virchows Archiv A

Scanning and Transmission Electron Microscopy of Ewing's Sarcoma of Bone (Typical and Atypical Variants)

An Analysis of Nine Cases

Antonio Llombart-Bosch and Amando Peydro-Olaya
Department of Pathology, Medical School of the University, Av. Blasco Ibañez 17, Valencia-10, Spain

Summary. Scanning electron microscopy (SEM) is of value for the differential diagnosis of Ewing's tumor of bone. Based upon 9 new cases which were observed with SEM and TEM (transmission electron microscopy), this paper puts into consideration, for the first time, the SEM ultrastructure of Ewing's sarcoma (both variants; typical Ewing's sarcoma and the large cell Ewing's sarcoma). Furthermore, a new case of vascular Ewing's sarcoma, studied with TEM, is discussed and included in the differential diagnosis with other round cell sarcomas of bone.

Both Ewing's sarcoma types evidence common ultrastructural characteristics, but the atypical variant (large cell type) shows a greater variation in cell size and contour. The cell surfaces displayed smooth structures, interrupted only by clusters of short, stub-like microvilli. Isolated cilia were also observed.

Variations in cell contour and size within the same tumour are also induced through intensive chemotherapy, as noted in one of our cases.

SEM seems to be suitable for the differentiation of Ewing's tumours from other primary malignancies of the bone marrow, as is the case of the so-called "reticulum cell sarcoma of bone" or malignant non-Hodgkin lymphoma.

SEM studies associated with TEM give further support to the mesenchymal origin of this neoplasm.

Key words: Ewing's sarcoma – Transmission electron microscopy (TEM) – Scanning electron microscopy (SEM)

Scanning electron microscopy (SEM) has provided very decisive information on the general morphology of bone cells and tissues, particularly in the bone marrow, but very few studies until now have been made on its neoplastic derivatives, especially bone sarcomas. Among these, the round cell sarcomas of bone seem to be an appropriate subject for analysis with SEM, owing to their homogeneous cell distribution and to the almost complete lack of stroma.

Offprint request to: Llombart-Bosch at the above address

0340-1227/83/0398/0329/$03.60

Within the round cell sarcomas of bone, Ewing's sarcoma (Es) constitutes a tumour type which still lacks a precise structural histogenetic derivation. Moreover, the existence of typical and atypical variants (large cell Es, vascular type) as described by Dahlin (1978) and Llombart-Bosch et al. (1978) opens new ways into the nature and histogenesis of this neoplasm.

The purpose of this paper is to present further insights into the ultrastructure of this tumour using TEM and SEM. Thus we have collected 9 new cases from our files, in which typical and atypical variants of the tumour were included.

Patients and Methods

A total of nine cases diagnosed as Es provided the material for this study. Table 1 is a summary of the major clinical and pathological findings. The primary sites of the tumours are also given. Three of the 9 cases arose in the upper trunk; the rest were located in the pelvis (2 cases) and lower extremities (4 cases). The patients (♂=6 and ♀=3) ranged from 9 to 20 years of age at time of diagnosis. Generally the initial symptoms presented were pain and swelling, fever, and anemia. In 5 cases the tumours extended into the soft tissues, revealing firm masses of variable size, located within the deep subcutaneous tissues. In all cases Roentgenograms showed a bone involvement by the tumoural mass. Furthermore, in 5 cases metastasis was already present at diagnosis time, affecting lung, pleura, liver, and other bone sites, giving a multicentric appearance to the neoplasm.

Three of the nine cases were diagnosed as "atypical Ewing's sarcoma"; two cases (6 and 9) belonged to the large cell variant, and case 3 was a vascular type of Es, on which SEM could not be performed. Both large cell Ewing's sarcomas showed metastasis at diagnosis time and a very poor response to therapy.

All the patients were submitted to similar treatment, including the multidisciplinary approach proposed by Rosen et al. (1978) with radiation therapy, maintenance chemotherapy (T2 protocol) and in some cases intensive induction chemotherapy (T6 protocol); case 9, moreover, was submitted to surgery.

Small fragments of the 9 tumours were collected at the time of surgery. All were classified as Es with light microscopy. Smears were performed for cytology and cytochemistry. Tumour tissue was sliced immediately into 1–2mm-thick sections and processed for light microscopy, and for SEM and TEM. Two cases were processed for in vitro studies with tissue culture. Specimens for light microscopy were fixed in 10% buffered formaline, processed routinely and stained with hematoxilin-eosin, Gomori's impregnation, Masson's trichromique and PAS with and without diastase digestion for glycogen. PAS technique was performed simultaneously in smears. Several histochemical techniques were employed for cytochemical characterization of the neoplasm.

Tissue for TEM was cut into small blocks and immersed in 2.5% gluteraldehyde in 0.1 phosphate buffer solution (pH 7.4) for 2 h, then postfixed in 2% osmium tetroxide for 2 h. The specimens were dehydrated with a graded series of alcohol and propylene oxide, embedded in Epon and cut into semi-thin sections with glass knives and stained with toluidine blue for light microscopy. Ultrathin sections were prepared on the selected fields in an LKB ultramicrotome, and then doubly stained with lead citrate and uranyl acetate and examined at 60–80 KV in a Jeol 100 B electron microscope.

Fragments for SEM were trimmed into small squares of 1 cm^2 and then processed with the tannin-osmium impregnations method of Murakami (1974). The specimens kept in gluteraldehyde were washed in buffer solution for a few minutes, then transferred to a mixed solution of 2% glycine, 2% sucrose and 2% sodium glutamate; secondly, to 2% tannic solution, and finally to a 2% osmium tetroxide solution. Dehydration was performed with either a graded ethanol or acetone series. The samples were immersed in isoamyl-acetate and quench-frozen in Freon-12, cooled with liquid nitrogen; immersed in cooled isoamyl-acetate and critical point dried using CO_2 in a Sorvall apparatus model. The dried samples were mounted on stubs, using conducting silver paste and coated with a thin layer of carbon and gold in a

Table 1

Number	Type	Age	Location		Treatment	Follow-up data	
						Metastasis	Last known status
1	tE	17 ♀	pelvis (ischium, pubis and soft tissue)		RT: 50 Gy and CT	none	alive and NED (2 years)
2	tE	20 ♀	9th rib	L	RT: 50 Gy and CT	multiple (lung, bones)	death (3 months)
3	atE (vascular)	9 ♀	fibula (upper third and soft tissue)		RT: 60 Gy and CT	none	alive and NED (14 months)
4	tE	10 ♂	femur (diaphisis and soft tissue)	L	RT: 50 Gy and CT	none	alive and NED (12 months)
5	tE	10 ♂	scapula (and soft tissue)	R	RT: 50 Gy and CT	multiple (lung)	death (6 months)
6	atE (large cell)	15 ♂	pelvis (and soft tissue)		CT	multiple (and residual tumor)	death (2 months)
7	tE	11 ♂	fibula (lower third and lung metastasis)		RT: 60 Gy and CT	multiple (bone, lung, liver)	under treatment alive (6 months)
8	tE	14 ♂	tibia (upper third)		RT: 60 Gy and CT	none	under treatment alive and NED (5 months)
9	atE (large cell)	16 ♂	9th rib (pleura and soft tissue)	L	surgery and CT	pleural effusion	under treatment alive (3 months)

Symbols: tE = typical Ewing's sarcoma; atE = atypical Ewing's sarcoma; RT = radiotherapy; CT = chemotherapy (Rosen et al. 1978); NED = no evidence of tumor; L = left; R = right

vacuum evaporator (HUS-2, Hitachi). The samples were then studied and photographed with a Phillips SEM-500 scanning electron microscope.

Results

Optical Microscopy

As previously mentioned, because of the lack of a precise structural histogenetic classification, the histological features are at present the only valid criteria for classification of this neoplasm.

The typical Es was composed of closely-packed cells with round or oval nuclei and scanty, ill-defined cytoplasm. Two cell types could be distinguished; blastemal or principal, and dark, secondary ones. Glycogen, when present, appeared located in blocks within both cell types. The principal

cells possessed a fine and fairly diffusely-dispersed chromatin and one or two small nucleoli. No binucleated cells were seen. Mitosis was abundant. The dark, secondary cells were of a degenerative nature, and were irregularly scattered among the principal ones, transitional forms being visible in between. These dark cells were smaller, and had folded nuclei; the chromatin was condensed. Necrotic and pyknotic or karyolytic nuclei were not uncommon.

Fibrillar stroma were either absent or very sparse, with isolated reticular fibres of preferent perivascular origin. Furthermore, a fibrinous deposit and edema could be observed. Vessels were scanty and irregularly distributed. An endothelial hyperplasia could be seen in some tumors associated with thickened basement membranes. Close contacts have been described among hyperplastic endothelia and tumoral cells. Necrosis was abundant.

Atypical Es (large cell type): This tumor variant could be isolated through the presence of large principal cells which were provided with very prominent, large nuclei. These nuclei were round or oval in shape; occasionally binucleated cells could be seen. The chromatin was peripherally distributed and condensed. One or two bright nucleoli could be observed. Mitotic activity was high. The cytoplasm became much more prominent and eosinophylic, even when the cell borders were indistinct. In 3 other cases herein described, glycogen was demonstrably distributed in blocks surrounding the nuclei.

The large cells coexisted with smaller ones similar to those seen in the conventional Es, within the same fields. The size of some cells was even twice that of those of the classic type of tumor. Texture and distribution of the secondary, dark cells were similar to those previously described.

A further difference between both tumor variants was the more elaborated reticular network which adopted, in this cell variant, a basketlike distribution (reticuline en corbeille). Necrosis was also abundant.

We wish to point out how all these morphological variations seen at optical level were not of a degenerative nature, and must therefore be distinguished from histological artifacts due to poor fixation, or to the presence of necrotic fields.

Transmission Electron Microscopy

Most of the TEM findings on Es have been extensively discussed by other authors (Friedman and Gold 1968; Friedman and Hanaoka 1971; Hou-Jensen et al. 1972; Rice et al. 1973; Incze et al. 1977; Povysil and Matejovsky 1977) as well as by ourselves (Llombart-Bosch et al. 1970; Peydro-Olaya and Llombart-Bosch 1972; Llombart-Bosch and Blache 1974; Llombart-Bosch et al. 1978). We have paid particular attention to the atypical variants of this tumor – large cell Es (Llombart-Bosch 1978; Llombart-Bosch et al. 1978) and to the vascular type (Llombart-Bosch et al. 1980, 1982). Review articles are at present in press (Llombart-Bosch et al. 1982; Llombart-Bosch and Peydro-Olaya 1982).

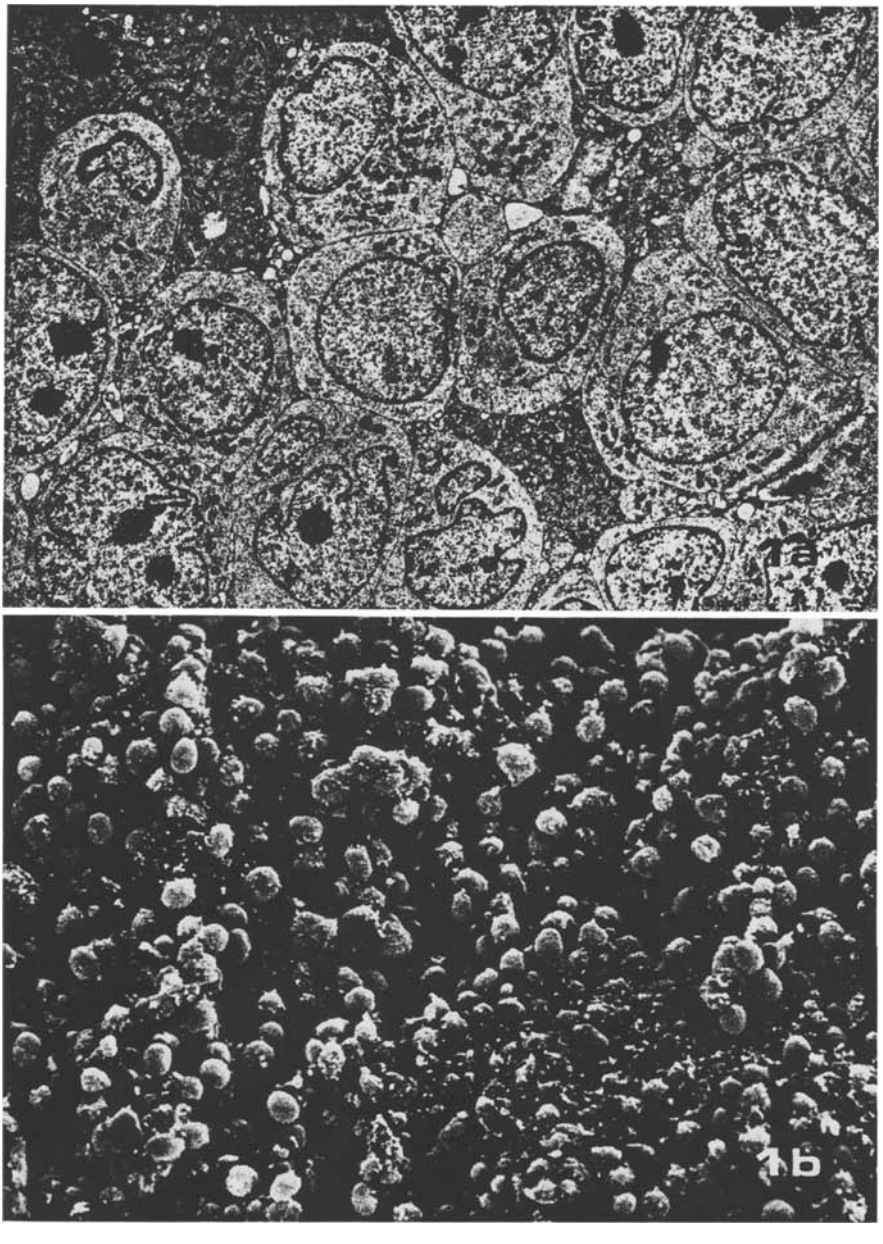

Fig. 1a, b. Typical Ewing's sarcoma of bone. **a** TEM general view of the neoplasm with grouping of principal blastemic cells and degenerative secondary ones (dark cells). Absence of stroma. Note the close intercellular contacts among the cells. In present case no glycogen is visible within the cytoplasm, which is poor in organelles. × 3,000. **b** SEM image of the neoplasm. The cells are homogeneous and grouped in small clusters configurating pseudo-rosette-like figures. Scarce stroma with some fibrin deposits. × 300

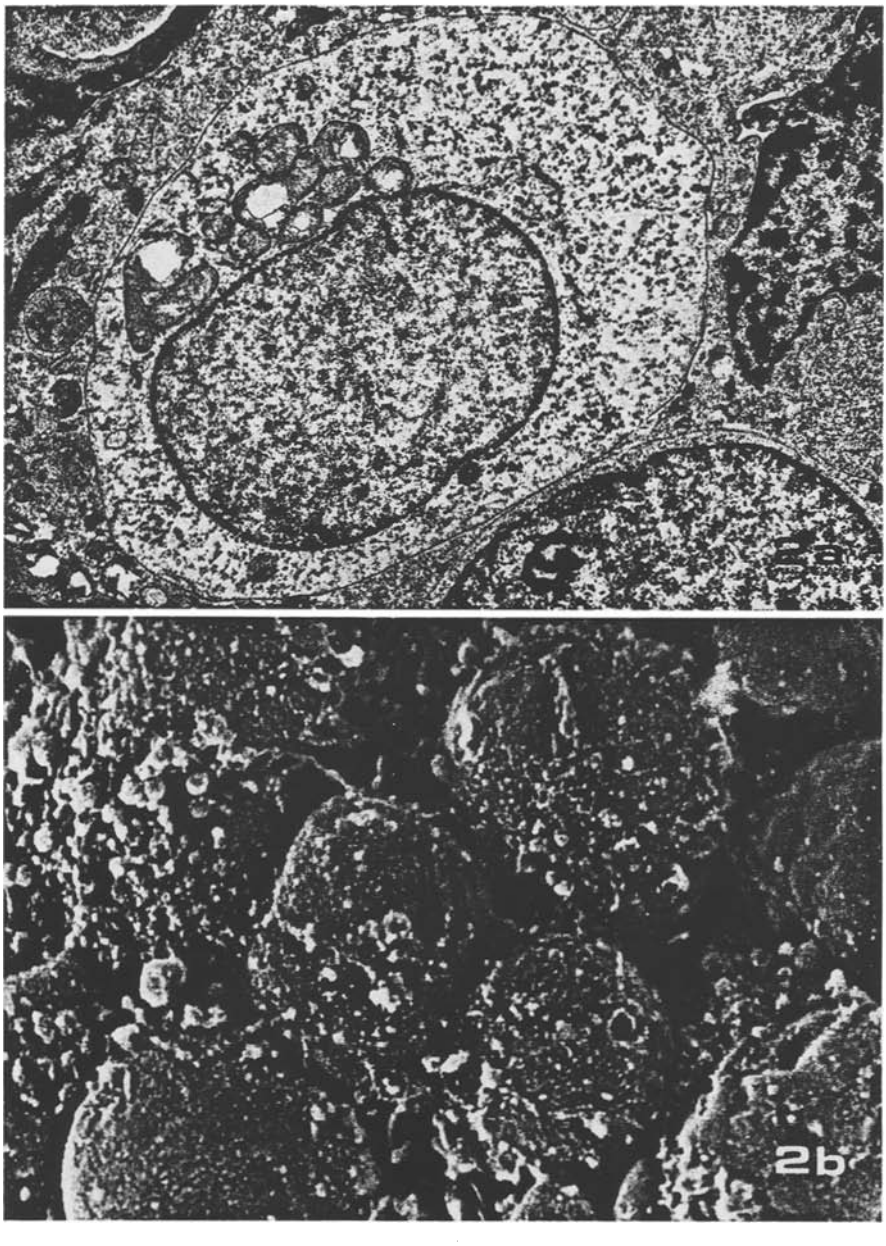

Fig. 2a, b. Typical Ewing's sarcoma of bone. **a** TEM detail of a neoplastic principal cell with diffuse glycogen deposits within the cytoplasm. The nucleus is round with a finely dispersed chromatin. ×10,000. **b** SEM analysis of a group of principal cells in the same case. The cells are round or polygonal. Surfaces are relatively smooth with some minute projections. A fibrin-like material covers the surface. ×4,000

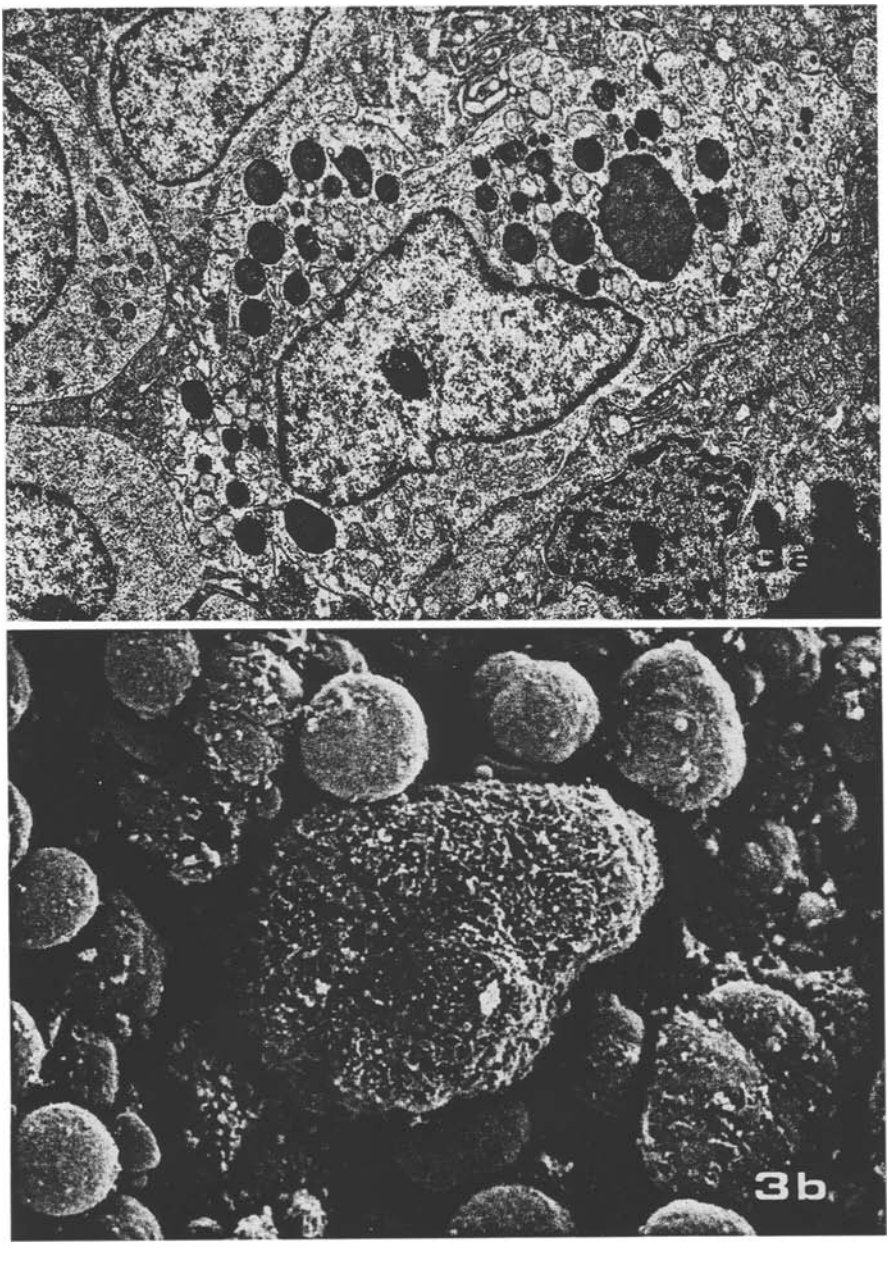

Fig. 3a, b. Typical Ewing's sarcoma: Comparative view (**a**) TEM and (**b**) SEM of a macrophage located between tumoral cells. Note at TEM level the abundance of secondary lysosomes within the cytoplasm and rough surface with microvilli. The surface of the macrophage and of several tumoral cells is seen at (**b**). The distinction of cell surfaces is notable when comparing tumoral principal cells and macrophagic ones. **a** ×8,000. **b** ×2,000

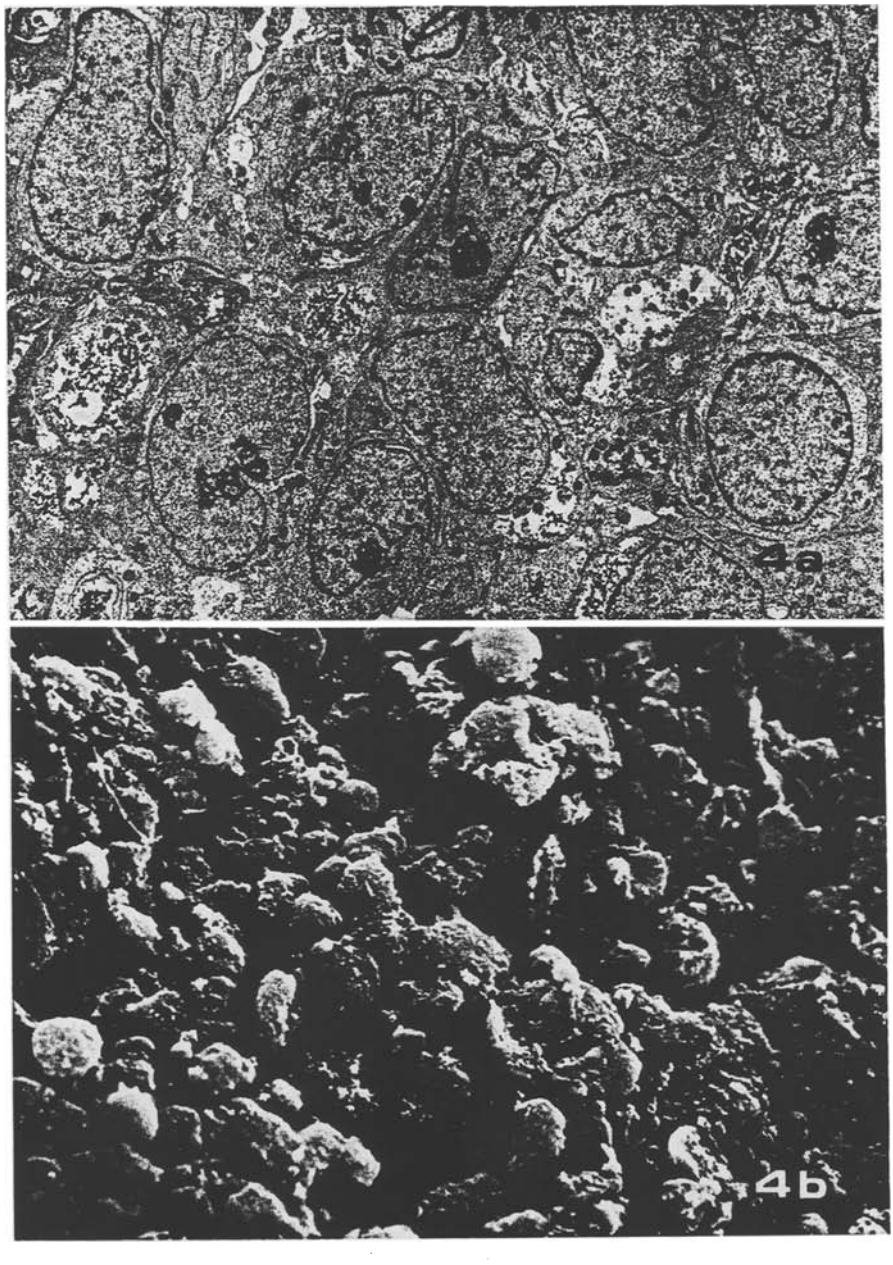

Fig. 4a, b. Large cell Ewing's sarcoma. **a** Cellular size and contour at TEM. Note the marked nuclear irregularities, and the presence of large nucleoli. Present case shows abundant glycogen in block deposits within the cytoplasm. ×3,000. **b** SEM overview of the neoplasm. Cells are isolated from each other but heterogeneity is more evident when compared with the typical Ewing's sarcoma, and the size and the shape of the cells are more irregularly delimited. Stroma is more abundant. ×600

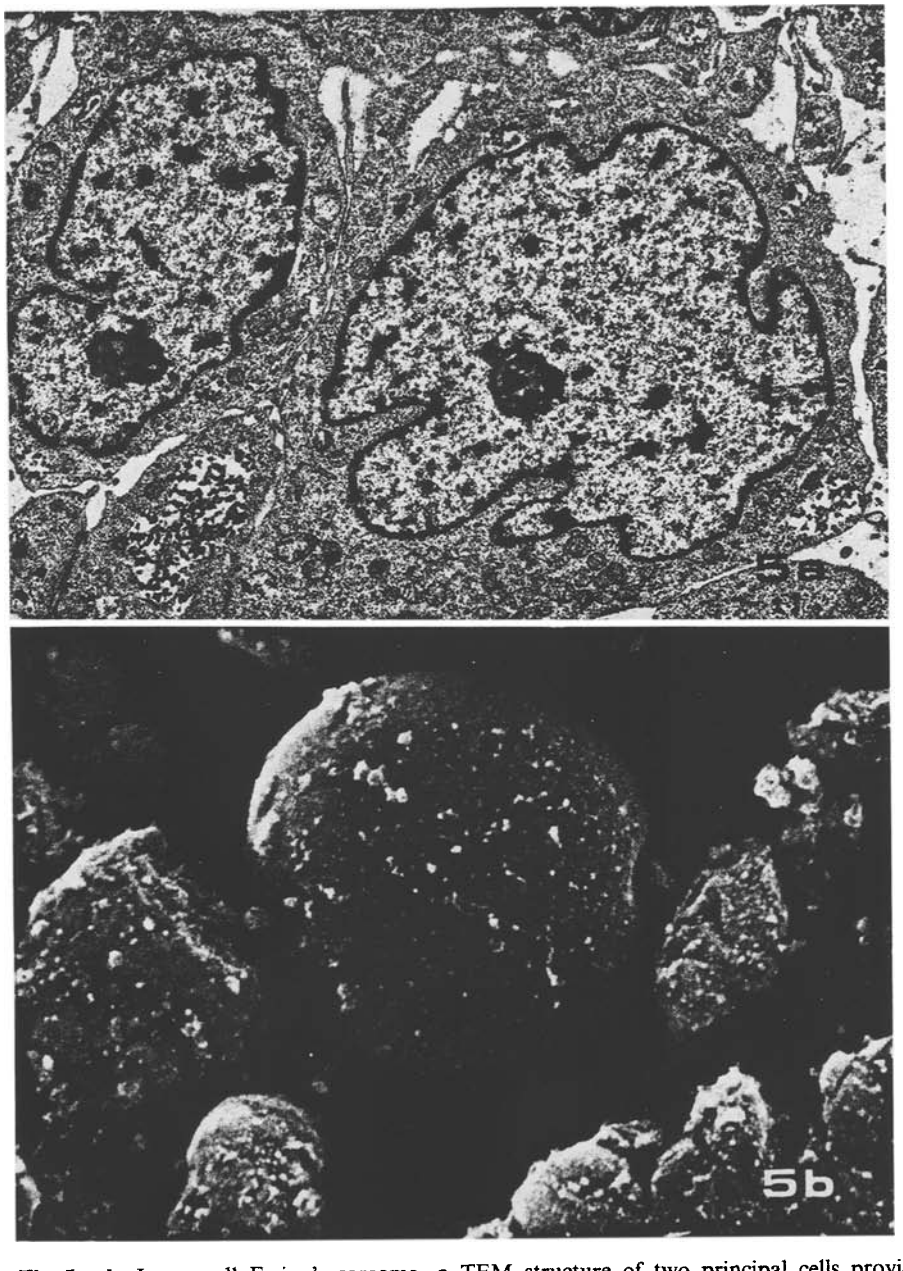

Fig. 5a, b. Large cell Ewing's sarcoma. **a** TEM structure of two principal cells providing a more mature appearance. Nuclear contours are irregular with infoldings. Chromatin appear in fine masses at the periphery. Glycogen deposits in the cytoplasm. × 7,500. **b** SEM of a large cell located between the small ones. Surface is flat with occasional minute depressions. Fibrin deposits and globules cover the surface. × 5,000

Typical Es was made up of principal blastemic cells of an undifferentiated nature and secondary, dark cells of a different electron density. Both cell types were closely packed, with sparse stroma on which fibrine deposits could be observed. Principal cell size was about 12–14 μ being roughly spherical or polygonal to elongated, with isolated processes. The cells were surrounded by a single layer plasma membrane, which showed some discontinuity and ruptures. There were rudimentary cell attachments with large local thickenings of opposed membranes and desmosome-like plaques of very imperfect nature. Nuclei appeared round to oval, occasionally indented with membrane blistering; their chromatin was finely dispersed. One or two nucleoli were present. Cytoplasm was clear with paucity in organelles, configurated by groups of mitochondria which were round or elongated, partially disrupted and with sparse and stubby cristae. The rough endoplasmic reticulum was sparse and a moderate number of ribosomes was usually scattered throughout the cytoplasm. We have seen very isolated bundles of filaments with no particular organization, irregularly distributed within the cytoplasm.

The dark cells appeared conglomerated in groups or nests or isolated among the principal ones, but no attachment sites existed in between. The cell contours were irregular and not well-delimited, the plasma membrane being disrupted and fragmented. The cell size was about 8–10 μ and the shape elongated or stellated but never spherical. The nucleus was oval, irregularly indented, and with great variation in shape and size; its chromatin was very dense and conglomerated. No mitosis was seen.

We have observed transitional images between typical immature principal cells and secondary ones. The latter were interpreted as degenerative types of the former.

Cells in the atypical variant (large cell Es) were very similar to the former but size and shape of the cells may be larger and better defined (about 15–20 μ in size) and some were even binucleated. Cell shape was spherical to polygonal and the plasma membrane was usually well-delineated and provided with imperfect desmosomes or large desmosome-like attachment plaques. The nuclei were round or oval with blistering and deep indentations, being more irregular than those seen in typical Es. The chromatin was peripherally condensed and the nucleoli were highly prominent. In the cytoplasm several lysosomes were present, isolated or in small clusters bordering the Golgi fields, which were numerous. No phagosomes were seen. Several REG profiles were also seen and the lipid vacuoles were in contiguity to blocks of glycogen and filaments. Glycogen was present in some cells, being less abundant than in typical Es. The existence of dark cells was similar to that observed in the typical variant.

Vessels in this variant were more numerous and showed prominent membrane thickenings and highly hyperplastic endothelia. The interstices were filled with fibrine-like material and reticular fibres, displaying a dense pattern which is not usually seen in its typical counterpart.

Particular attention should be paid to Case 6, which was studied at TEM and SEM with specimens obtained just before the death of the 15

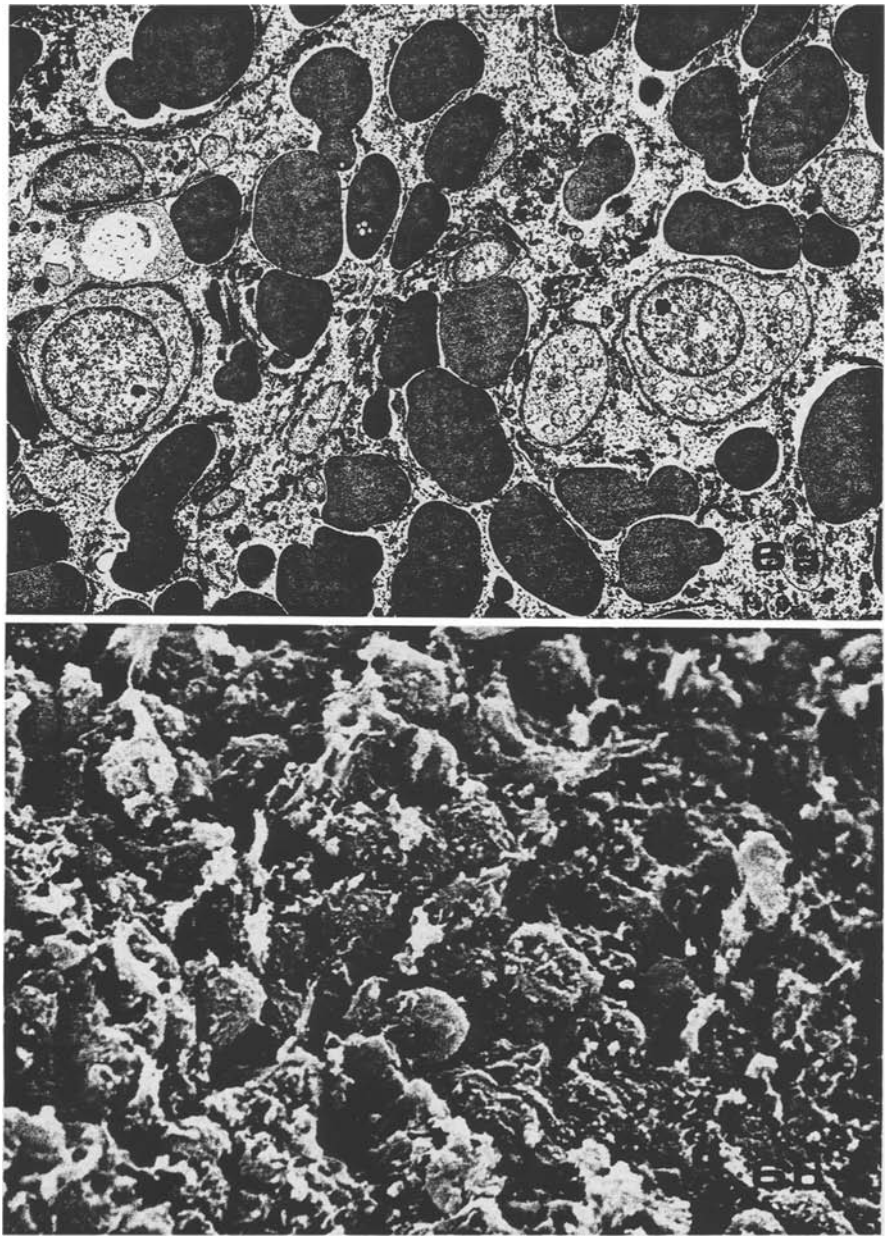

Fig. 6a, b. Atypical Ewing's sarcoma, induced through intensive chemotherapy (case No. 6). **a** Tumoral cells are isolated and surrounded by erythrocytes in hemorrhagic plaques. Abundant cell debris and histiocytes. × 3,000. **b** SEM general view of the same tumor mimicking those structures seen in the large cell variant of Ewing's sarcoma. Cell variations in size, shapes and surfaces are numerous. Abundant fibrin deposits and fibrillar network with cellular debris in necrosis. × 750

year-old boy suffering from an ischiatic tumor which showed high resistance to radio- and chemotherapy. These neoplasms were highly necrotic, but cells survived among fibrine and edematous-like material. Principal cells were large; in some cases polyploid with large, oval or elongated shape (about 25 μ in size). A macrophagic activation was present. Most of the tumoural cells were not destroyed by the treatment and divided actively.

Atypical vascular Es (Case 3) is the third published Ewing's sarcoma with vascular features. Previous cases were discussed by ourselves (Llombart-Bosch et al. 1980; Llombart-Bosch et al. 1982). Such cases are extremely uncommon. In this new one only a TEM study could be performed. The cells in this tumour variant were well-differentiated and showed some endothelial characteristics, such as clear vacuolated cytoplasm, abundant pinocytic vacuoles and well-developed cytoplasmic contacts. Moreover, numerous bundles of filaments were present, similar to those seen in the endothelium. Imperfect Weibel Palade bodies could be detected. These cells were arranged in sheets or cords with slits and pseudo-spaces. Some were filled with erithrocytes, but no true capillaries were observed. The stroma showed small capillaries covered by highly hyperplastic endothelia but with an amorphous basement membrane which separated lumina from the immediately neighbouring tumour cells. Pericytes were seen in intimate contact with neoplastic cells.

Scanning Electron Microscopy

Our SEM observations correspond with those of TEM. The tumoral cells appeared homogeneously distributed in small clusters, being spherical in shape and tenuously attached to each other, with only a small part of their circumference in contact. Other fields adopted a grape-like texture on which the cells clustered, forming pseudo-rosettes. Moreover, there were sheets or compact nests of cells intimately attached, with large contacts of their surfaces. All these contacts were uniformly in contiguity. The stroma was very scarce and only some elongated fibres were observed. The cells adopted a perivascular distribution.

Cell size was very homogeneous, with spherical or polygonal shapes. Some cells were slightly elongated, and showed focal surface flattening or depressions. In some cases the cells were more individually scattered or irregularly dumped together, being round or spindle-shaped.

The surface morphology of all Es cells was very similar, irrespective of tumour location or specimen investigated, although occasional, slight variation in surfaces could be detected from case to case. The general morphology, however, was very similar in all sites and all cases.

Clear-cut differences between principal, round or polygonally shaped cells and secondary, dark ones as revealed by TEM could only occasionally be detected with SEM. Secondary cells appeared scattered and mixed with the large, round spherical ones, which were considered as principal cells. Moreover, they varied in shape and contour, being elongated and with irregular limits. Some spindle-shaped cells were of a degenerative nature.

The sarcomatous cells possessed relatively smooth surfaces; only occasional projections or minute depressions were demonstrable, and better seen at higher magnifications. Nevertheless some surface variations in structure existed. In some round cells the surface was occupied by short, stubby microvilli of 0.1–0.3 μ in length, which were somewhat loosely-spaced and located in groups or in continuity to focal surface flattening or depressions of their surfaces. Shaggy microvilli were exceptionally seen in some principal cells; more commonly cytoplasmic projections were seen. Cell-to-cell contact induced lengthening of the cell surface and a polygonal cell shape. Membrane contacts were narrow, and contiguous cells were attached by stub-like microvilli. No ruffled membranes were seen in the neoplastic cells.

Groups of tumoural cells were covered with fibrine-like material, which configurated a tiny network around them. The vessels, being scattered in the stroma, were irregularly distributed. They were of capillary type, with fine endothelia lining their internal surface. No basement membrane could be identified isolating the vessels from the neoplastic cells which surrounded them in a very intimate way. Thick vessel walls with large, elongated endothelial cells were also observed. In some cases sarcomatous cells infiltrated the vascular wall, being situated within its lumina.

The stroma was filled with numerous erithrocytes and isolated lymphocytes, which were small and showed long, finger-like microvilli as well as stub-like ones. Large macrophages possessed irregular shapes and were twice the size of the principal cells. Their surfaces were flat, with finger-like projections and some ruffled membranes.

No striking differences were detected when comparing typical Ewing's sarcoma with its large cell variant by SEM. The most outstanding features of this atypical variant were the following:

The neoplasm maintained a homogeneous cell pattern distributed in clusters, sheets, or nests, with little or no stroma. The cells were round or spherical with light contacts, or adopted a flattened polygonal contour, with large, narrow contacts of the cell surface which were finely delimited. The great variation in cell size was one of the most outstanding features; small (about 15 μ) and large (25–30 μ in size) cells cohabitated within the same fields; but broad areas of the tumour were exclusively composed of large cells. Some of these latter possessed an ovoid, elongated configuration. The fusiform shape of many cells continued to be evident, and the rounded cells decreased, the flattened ones being successively plentiful.

The surface morphology in the large cells mimicked that seen in its typical variant. Most round cells displayed a smooth surface interrupted only by clusters of short, stub-like microvilli, but no ruffled membranes similar to those in monocytes could be seen. More numerous projections existed in those cells which adopted a polygonal and flattened configuration. The plasma membrane showed numerous, short stub-like microvilli which covered the surface homogeneously, and close contacts could be detected between neighbouring cells. Even when the stroma was more fibrillar, no marked differences could be detected when compared with the classic Ewing's sarcoma.

The most marked differences in tumour texture and cell shape and size were observed in Case 6 (treated with intense chemotherapy until just before death). The cells were included within a fibrillar and fibrinous stroma, which was very haemorrhagic and mixed with blood cells and macrophages. In some fields the tumoural cells were enmeshed within the fibrinous component, which isolated the cells in groups. A very rich plasmatic exhudation delimited cavities in which pleomorphic tumour cells were embedded.

Variations in shape of the cells allowed a more heterogeneous pattern which was in accordance with the presence of giant cells of sarcomatous nature, similar to those seen with TEM. The surfaces of the giant cells were smooth or with very tiny, stubby microvilli.

Discussion

The main object of this paper is to stress the value of SEM in the diagnosis and histogenetic study of Ewing's tumors. Two new cases of large cell Ewing's tumors are also presented, studied with TEM, thus adding new support to previous work by our group (Llombart-Bosch et al. 1978; Llombart-Bosch et al. 1982) and others (Dahlin 1978; Nascimento et al. 1980). No TEM study of large cell Es primary to bone has thus far been described following our initial presentation, but several authors have discussed the morphology of extraskeletal Es with TEM, which shares some close morphological points in common with our cases.

The clinical aspects of these tumours (compiled in Table 1) are in agreement with other authors (Nascimento et al. 1980) as well as with our own findings following a recent review of 233 Ewing's tumours (Llombart-Bosch et al. 1982), 17 of which belonged to the large cell variant, and 3 were of angiomatous nature. Large cell Ewing's sarcoma is present mainly in adolescents, with a clear male predominance. No differences in anatomical locations were detected in our cases. Prognostic factors are dependent upon the kind of therapy employed, but generally results are poor and prognosis is less favourable than that attained with its homologous counterpart (i.e. typical Ewing's sarcoma). It is therefore of importance for the clinic to differentiate both cell variants of the neoplasm.

Furthermore, in this paper we also analyse a TEM study of a vascular variant of Es. Two previous cases have already been published by ourselves (Llombart-Bosch et al. 1980, 1982). At present there is not enough experience on this neoplasm for general conclusions but from a histological point of view there seem to be cross-links between Es and haemangioendothelioma of bone, actualizing the old theory which supported a vascular origin for Ewing's tumors (Ewing 1921, 1939).

SEM has been used mainly in research, although its potentiality for diagnostic pathology has been proven in very diverse types of tumors (Lupulescu and Boyd 1972; Gonda et al. 1976; Dionne and Wang 1977; Roath et al. 1978) mainly in epithelial neoplasms (Fenoglio et al. 1975; Incze et al. 1977; Tannenbaum 1979) and in haematopoyetic malignant proliferations (Polliack et al. 1975; Katayama and Schneider 1977; Müller-Hermelink and

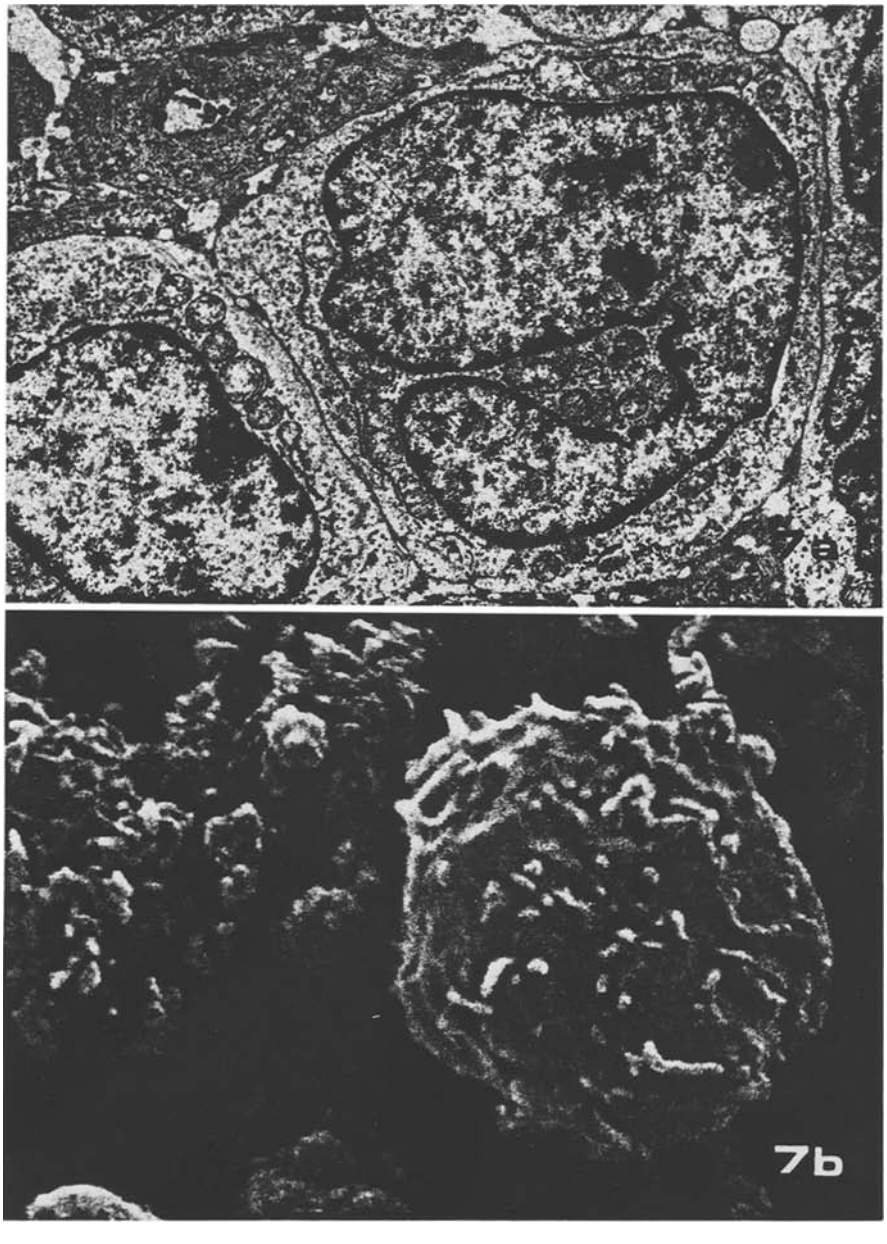

Fig. 7a, b. Histiocytic non-Hodgkin lymphoma of bone (reticulum cell sarcoma). **a** Cell to cell contacts and variations in size of cells are characteristic for this tumor. Immature "histiocytes" show a monocytic appearance. ×10,000. **b** The cell surface at SEM level exhibits ruffle-like and rough-surface foldings, which are always absent in Ewing cells. ×6,000

Müller-Hermelink 1977; Polliack 1978; Polliack 1979; Skinnider 1979; Sokol et al. 1979; Polliack et al. 1981) but no SEM findings are presently available on malignant round cell sarcomas of bone.

The first question to be established is to know whether Es cells possess specific morphological features in SEM, which would make its identification possible when compared with other round cell tumours of bone. Based upon present investigations the histological and cytological criteria together with this method seem to be highly suitable in order to differentiate Ewing's tumours and the atypical variant (large cell Es) from other malignancies such as reticulum cell sarcoma (non-Hodgkin malignant lymphoma of histiocytic type) and malignant lymphoma in bone (types other than the histiocytic variant).

The degree of clustering and cohesiveness of the cells, associated to the homogeneity of the cell population and the absence of stroma are typical characteristics of Ewing's sarcoma. Moreover, the shape and homogeneous size of the cells are almost specific for this tumour type, not being visible in malignant lymphoma (Roath et al. 1978) or in malignant histiocytic sarcoma. Our own SEM observations of a malignant histiocytic "reticulum sarcoma of bone" showed a monocytic-macrophagic cell appearance with marked cell irregularities, with variable size and shape of the neoplastic cells. Histiocytes of monocytic origin exhibit mainly ruffle-like and rough-surface foldings, whereas lymphocytes typically show short stub-like microvilli or a smooth surface.

Large cell Es shares some structural characteristics of its homologous classic variant, but is also in full accordance with TEM observations previously discussed. Large cells in atypical Es may be present in isolated form or in clusters configurating large fields of the specimen investigated. This fact gives support for a common histogenesis and nature of both tumour types. The variations in form and size of the Ewing's sarcoma can also be induced through intensive chemotherapy, as we have observed in one of our cases (No. 3) and was already mentioned by Telles, Rabson and Pomeroy (1978) on an autopsy study performed on 26 cases. Tumours at autopsy frequently have increased pleomorphism and increased numbers of giant cells. Moreover, SEM studies associated to previous findings at TEM level give more solid support to the mesenchymal origin of this neoplasm.

References

Dahlin DC (1978) Bone tumours; General aspects and data on 6,221 cases (3rd ed.) Charles C Thomas, Springfield, Ill.

Dionne GP, Wang NS (1977) A scanning electron microscopic study of diffuse mesothelioma and some lung carcinomas. Cancer 40:707–715

Ewing J (1921) Diffuse endothelioma of bone. Proc NY Pathol Soc 21:17–24

Ewing J (1939) A review of the classification of bone tumors. Surg Gynecol Obstet 68:971–976

Fenoglio CM, Ferenczy A, Richart RM (1975) Mucinous tumors of the ovary. Ultrastructural studies of mucinous cystadenomas with histogenetic considerations. Cancer 36:1709–1722

Friedman B, Gold H (1968) Ultrastructure of Ewing's sarcoma of bone. Cancer 22:307–322

Friedman B, Hanaoka H (1971) Round-cell sarcomas of bone. A light- and electron-microscopic study. J Bone Joint Surg 53-A:1118–1136

Gonda MA, Aaronson SA, Ellmore N, Zeve VH, Nagashima K (1976) Ultrastructural studies of surface features of human normal and tumour cells in tissue culture by scanning and transmission electron microscopy. J Natl Cancer Inst 56:245–263

Hou-Jensen K, Priori E, Dmochowski L (1972) Studies on ultrastructure of Ewing's sarcoma of bone. Cancer 29:280–286

Incze JS, Lui PS, Strong MS, Vaughan CW, Pais Clemente M (1977) The morphology of human papillomas of the upper respiratory tract. Cancer 39:1634–1646

Kadin ME, Bensch KG (1971) On the origin of Ewing's tumour. Cancer 27:257–273

Katayama I, Schneider GB (1977) Further ultrastructural characterization of hair cells of leukemic reticuloendotheliosis. Am J Pathol 86:163–174

Llombart-Bosch A (1978) Sobre la heterogeneidad del sarcoma de Ewing oseo. Caracterizacion ultraestructural de dos variantes morfologicas. Res Esp Cir Ost 13:303–322

Llombart-Bosch A, Blache R (1974) Ueber die Morphologie und Ultrastructur des Ewing-Tumors. Ver Dtsch Ges Pathol 58:459–466

Llombart-Bosch A, Blache R, Peydro-Olaya A (1978) Ultrastructural study of 28 cases of Ewing's sarcoma: typical and atypical forms. Cancer 41:1362–1373

Llombart-Bosch A, Blache R, Peydro-Olaya A (1982) Round cell sarcomas of bone and their differential diagnosis (with particular emphasis on Ewing's sarcoma and reticulosarcoma). A study of 233 tumours with optical and electron microscopical techniques. Pathol Ann 1982-II

Llombart-Bosch A, Peydro-Olaya A (1982) Ultrastructural characterization of round cell sarcomas of bone with transmission and scanning electron microscopy. Acta Medica Portuguesa [in press]

Llombart-Bosch A, Peydro-Olaya A, Gomar F (1980) Ultrastructure of one Ewing's sarcoma of bone with endothelial character and a comparative review of the vessels in 27 cases of typical Ewing's sarcoma. Pathol Res Pract 167:71–87

Llombart-Bosch A, Peydro-Olaya A, Lopez-Fernandez A, Zuzuarregui C (1970) Sur les sarcomes réticulaires de la moelle osseuse type Ewing. Etude optique histochemique et electronique de deux cas. Ann Anat Pathol 15:431–453

Llombart-Bosch A, Peydro-Olaya A, Pellin A (1982) Ultrastructure of vascular neoplasms. A transmission and scanning electron microscopical study based upon 42 cases. Pathol Res Pract 174:1–41

Lupulescu A, Boyd CB (1972) Lung cancer. A transmission and scanning electron microscopic study. Cancer 29:1530–1538

Müller-Hermelink U, Müller-Hermelink HK (1977) Scanning electron microscopic investigations of acute leukemia. Virchows Arch [Cell Pathol] 23:227–236

Murakami T (1974) A revised tannin-osmium method for noncoated scanning electron microscope specimens. Arch Histol Jpn 36:189–193

Nascimento AG, Unni KK, Pritchard DJ, Cooper KL, Dahlin DC (1980) A clinicopathologic study of 20 cases of large-cell (atypical) Ewing's sarcoma of bone. Am J Surg Pathol 4:29–36

Peydro-Olaya A, Llombart-Bosch A (1972) Sarcoma de celulas redondas de la medula osea. Un estudio histoquimico y microscopico-electronico. Sangre (Zaragoza) 17:363–377

Polliack A (1978) Surface morphology of lymphoreticular cells: review of data obtained from scanning electron microscopy. Recent Results Cancer Res 64:66–93

Polliack A (1979) Scanning electron microscopy and the surface morphology of human leukocytes: current status. Isr J Med Sci 15:629–638

Polliack A, McKenzie S, Gee T, Lamken N, de Harven E, Clarkson BD (1975) A scanning electron microscopic study of 34 cases of acute granulocytic, myelomonocytic, monoblastic and histiocytic leukemia. Am J Med 59:308–315

Polliack A, Prokocimer M, Or R, Korkesh A, Leizerowitz R, Ben-Bassat H, Gamlier H (1981) Use of multiparameter studies and scanning electron microscopy in the interpretation and attempted correlation of surface morphology with cell type in 135 cases of human leukemias. Cancer Res 41:1171–1179

Povysil C, Matejovsky Z (1977) Ultrastructure of Ewing's tumor. Virchows Arch [Pathol Anat] 374:303–316

Rice RW, Cabot A, Johnson AD (1973) The application of electron microscopy to the differential diagnosis of Ewing's sarcoma and reticulum cell sarcoma of bone. Clin Orthop 91:174–185

Roath S, Newell D, Polliack A, Alexander E, Lin PS (1978) Scanning electron microscopy and the surface morphology of human lymphocytes. Nature 273:15–18

Rosen G, Caparros B, Mosende C, McCormick B, Huvos AG, Marcove RC (1978) Curability of Ewing's sarcoma and considerations for future therapeutic trials. Cancer 41:888–899

Skinnider LF (1979) Scanning electron microscopic study of follicular lymphoma. Arch Pathol Lab Med 103:276–278

Sokol RJ, Durrant TE, Lambourne CA, Hudson G (1979) Scanning electron microscopy of exudative macrophages in malignant lymphoma. Scan J Haematol 22:129–140

Tannenbaum M (1979) Ultrastructural pathology of the human urinary bladder. In: Trump BF, Jones RT (eds) Diagnostic electron microscopy, vol 2. John Wiley & Sons, New York, Chichester, Brisbane, Toronto pp 221–267

Telles NC, Rabson AS, Pomeroy TC (1978) Ewing's sarcoma: an autopsy study. Cancer 41:2321–2329

Accepted September 30, 1982